Supplementary Methods

Cloning and protein expression

Homo sapiens DDB1 (residues 1-1140), *Gallus gallus* CRBN (residues 1-445) [for crystallography studies] and *Homo sapiens* CRBN (residues 1-442) [for all biochemical and biophysical assays] were cloned into pAC-derived vectors[1] (BD Biosciences PharMingen); recombinant baculoviruses were prepared according to the manufacturer's protocol. Proteins were expressed as N-terminal His_6 (DDB1), N-terminal StrepII or N-terminal His_6-tagged (CRBN, MEIS2) and N-terminal StrepII-BirA (CSN) fusion proteins in Hi-Five insect cells (Invitrogen).

For purification, cells were resuspended in lysis buffer containing 50 mM Tris-HCl pH 8.0, 200 mM NaCl, 0.25 mM TCEP (*tris*(2-carboxyethyl)phosphine), 1 mM PMSF, and 1 tablet/500 ml protease inhibitor cocktail (Sigma), and lysed by sonification. The lysate was clarified by ultracentrifugation and proteins purified using Strep-Tactin affinity purification or Ni-NTA affinity purification. Proteins were further purified by anion exchange chromatography (Poros 50HQ) using a 0 - 700 mM NaCl gradient. Size exclusion chromatography (SEC) (HiLoad 16/60 Superdex 200; GE Healthcare) in 50 mM HEPES pH 7.4, 200 mM NaCl and 0.25 mM TCEP yielded proteins without visible contamination (Coomassie-stained SDS-PAGE). The purified protein was concentrated using "Amicon Ultra" spin concentration devices, flash frozen in liquid nitrogen and stored at -80°C until further use.

For transient overexpression in HEK293T cells and stable cell line selection, *Homo sapiens* MEIS2 transcript variant d and *homo sapiens* CRBN and $CRBN^{YW/AA}$ were purchased as a Myc-DDK-tagged expression construct from Origene (RC208386L1, RC209794, pCMV6-entry). CRBN constructs were subcloned into a pCMV6-HA expression vector.

Compounds, enzymes and antibodies used

(*S*)-thalidomide, (*R*)-thalidomide and lenalidomide (*revlimid*) used for crystallization were generous gifts from NIBR (Cambridge, USA). (*S*)-Thalidomide for biochemistry was purchased from Sigma Aldrich (T150-100MG), lenalidomide (S1029) for biochemistry and pomalidomide (S1567) for crystallization and biochemistry from Selleckchem. All compounds were dissolved in DMSO at various concentrations. It was found that thalidomide exhibits limited stability in cell culture medium, which is not necessarily correlated to stability in human serum or cellular concentrations[29]. In accordance, we observed limited and varying stability for IMiDs especially in cell culture medium and therefore all compounds were frequently quality controlled by mass spectrometry and IMiD containing cell culture medium was always prepared immediately before use.

Ubiquitin activating enzyme E1 (UBA1, E-305), ubiquitin conjugating enzyme E2 (UbcH5a, E2-616; UbcH5b, E-622), ubiquitin (U100-H), N-terminal biotinylated ubiquitin (UB-560) and K_0 ubiquitin (UM-NOK) were purchased from Boston Biochem. Alexa647-Streptavidin and ProtoArray human protein microarray v5.0 were purchased from Life Technologies. Primary antibodies used included α-CRBN at

1:500 to 1:10,000 dilution (11435-1-AP, Proteintech), α-CRBN at 1:250 to 1:10,000 dilution (NBP1-91810, Novus), α-MEIS2 at 1:500 to 1:1,000 dilution (HPA003256, Atlas antibodies), α-MEIS2 at 1:250 to 1:500 dilution (H00004212-M01, Abnova), α-ERK2 at 1:3,000 to 1:5,000 dilution (sc-1647, Santa Cruz), α-DDK at 1:1,000 dilution (4C5, Origene), α-GAPDH at 1:5,000 dilution (G9545, Sigma), α-H4 at 1:5,000 to 1:10,000 dilution (ab10158, abcam). Secondary antibodies for infrared detection included donkey anti-mouse IRDye@800CW (926-32212, Li-COR), goat anti-rabbit Alexa680 (21076, Invitrogen), donkey anti-rabbit IRDye@800CW (926-32213, Li-COR) and goat anti-mouse IRDye@680RD (926-68070, Li-COR). Secondary antibodies were used at dilutions between 1:10,000 and 1:20,000. SK-N-DZ cells were purchased from ECACC (94092305, Sigma), M059J and M059K cells were kind gifts of B.A. Hemmnings (FMI).

Crystallization of hsDDB1-ggCRBN

Protein-thalidomide/lenalidomide co-crystals were obtained by mixing thalidomide or lenalidomide with purified hsDDB1-ggCRBN protein complex (12.5 mg/ml) in a molar ratio of 2:1 to 5:1. Initial screening was carried out using a Phoenix liquid handling robot (Art Robbins) and commercially available screens (Hampton; Qiagen). Initial hits were refined in a 24-well hanging-drop vapour diffusion setup by mixing 1 µl of protein solution (12.5 mg/ml) with 1 µl of reservoir solution (100 mM Na cacodylate, 80 mM NaH_2PO_4, 120 mM K_2HPO_4, 700-1,200 mM tri-Na citrate). Diffraction grade hsDDB1-ggCRBN-pomalidomide co-crystals were obtained under similar conditions. Crystals were transferred into cryo-solution (100 mM Na cacodylate, 80 mM NaH_2PO_4, 120 mM K_2HPO_4, 800 mM tri-Na citrate, 20 - 25% glycerol) and flash frozen in liquid N_2 for data collection.

Data were collected at beamlines X10SA and X06DA of the Swiss Light Source (Paul Scherrer Institute, Villigen, Switzerland) with a Pilatus 2M and Pilatus 6M detector, respectively. Data sets collected at a wavelength of 1Å were processed using XDS[2]. Additional scaling was carried out using AIMLESS and other programs of the CCP4 software suite[3]. A summary of the data processing and refinement statistics is provided in **Extended Data Table 1**.

Structure solution and model building

All crystals belonged to the space group $P3_221$ and contained one molecule in the asymmetric unit (AU). The structure of hsDDB1-ggCRBN bound to thalidomide was solved by molecular replacement using Phaser[4] with the BPA/BPC/CTD of DDB1 as search model. The BPA/BPC/CTD domains of DDB1 were fixed and the BPB domain searched with Molrep[5]. Rigid body refinement on DDB1 domains was carried out with phenix.refine[6]. The initial model of ggCRBN was iteratively built with Coot[7] and refined with phenix.refine[6] and autoBUSTER[8]. During model building, additional unaccounted density was observed close to a number of cysteines and the corresponding residues were tentatively assigned as dimethylarsoryl-L-cysteine in accordance with the crystallisation buffer containing 100 mM cacodylic acid. Crystallographic information files (CIF) for thalidomide, lenalidomide and

pomalidomide were generated using the Grade web server (globalphasing Ltd., Cambridge) and validated against structures from the Cambridge Structural Database[9]. Structures of lenalidomide- and pomalidomide-containing complexes were solved by molecular replacement with Phaser using the structure of hsDDB1-ggCRBN-thalidomide as a search model and refined with autoBUSTER and phenix.refine. Figures were generated with PyMol (DeLano Scientific, http://www.pymol.org). Molprobity was used to analyse model quality[10].

***In vitro* neddylation of CRL4^{CRBN}.**

In vitro neddylation of CRL4^{CRBN} complexes was carried out as previously described[11]. In short, 3.7 mg of purified CRL4A^{CRBN} was mixed with 50 µg E1 (NAE1/UBA3), 290 µg E2 (Ubc12) and 85 µg Nedd8 in a reaction buffer containing 50 mM Tris pH 7.5, 100 mM NaCl, 2.5 mM $MgCl_2$, 15 mM ATP and 0.5 mM DTT. The reaction was carried out at room temperature for 2h and full neddylation confirmed by SDS-PAGE analysis (**Extended Data Fig. 8j**). The neddylated CRL4A^{CRBN} complex was subsequently purified by size exclusion chromatography.

***In vitro* ubiquitination assays**

In vitro ubiquitination assays and CSN protection assays were carried out as described previously[12]. Final enzyme concentrations in the reaction mix were 15-20 µM ubiquitin, 0.04 µM E1, 0.07 µM CRL4^{CRBN} complex, 1 µM E2 (UbcH5a or UbcH5b) in 1x ubiquitin assay buffer[13]. CSN concentrations were 100– 400 nM as indicated. MEIS2 ubiquitination assays were performed following the same protocol with MEIS2 concentrations as indicated in the figures and legends. MEIS2 was treated prior to ubiquitination with 1,000 Units of lambda phosphatase (NEB) (1 unit hydrolyses 1 nmol of *p*-nitrophenyl phosphate in 1 min at 30°C) per 0.5 mg DDB1-CRBN (~ 3 nmol) lambda phosphatase (NEB) according to the manufacturer's protocol. Phosphorylation sites were mapped to residues Ser198, Ser206, Ser229 and Ser249 by mass spectrometry (data not shown) and dephosphorylation was confirmed. Dephosphorylation resulted in a shift on size exclusion chromatography towards a lower molecular weight fraction (data not shown), indicating possible disaggregation of the MEIS2 protein. We observed more efficient ubiquitination of dephosphorylated MEIS2 by CRL4^{CRBN} than the untreated control protein. Whether this was due to loss of phosphor moieties or to the observed disaggregation remains unclear. We also note that not all purified fractions were similarly efficient in CRL4^{CRBN} mediated ubiquitination and that freezing of the purified protein significantly decreased protein behaviour and CRL4^{CRBN}-mediated ubiquitination.

Compound-protein interactions by fluorescent polarisation

Cy5 conjugated thalidomide was used as a fluorescent probe. Increasing amounts of DDB1-CRBN complex were mixed with Cy5-thalidomide (10 nM) and incubated for 30 min at room temperature. Compound-protein interactions were monitored by change in fluorescent polarization of the Cy5 probe and the bound

fraction calculated as described in[14]. Data were plotted and fitted to a model for a single binding site with Origin (OriginLab).
Competitive titrations were carried out by mixing unlabelled compound with Cy5-thalidomide (10 nM) and hsDDB1-hsCRBN (100 nM). The fraction bound was plotted and the half maximal effective concentration (EC_{50}) calculated. EC_{50} values were converted to the K_i as previously described[15].

Immobilised Artificial Membrane (IAM) Chromatography
All HPLC experiments were carried out in gradient mode using 100% 50 mM ammonium acetate (pH 7.4) buffer as mobile phase A and 100% acetonitrile as mobile phase B. Immobilized artificial membranes (IAMs) consist of monolayers of phospholipid covalently immobilized on a silica surface, mimicking the lipid environment of a fluid cell membrane on a solid matrix. A previously described gradient method[16] was used to measure the CHI IAM7.4 values of all test drugs on a 10 cm x 4.6 mm, 10µm Regis IAM PC DD2 column (where the stationary phase support is immobilised phosphatidylcholine). The gradient was: 0 min/0 % B, 6.0 min/100 % B, 6.5 min/100 % B, 7.0 min/0 % B, 9.0 min/0 % B. The mobile phase flow rate was 1.0 mL/min. With a set of alkylphenone standards, (acetophenone, propiophenone, valerophenone, octanophenone) the gradient retention times can be converted to CHI IAM7.4, which approximates to an acetonitrile concentration at which an equal distribution of compound can be achieved between the mobile phase and IAM. The gradient method is an ideal way to assess phosphtidylcholine affinity as some samples retain extremely well on the phosphatidylcholine stationary phase and are extremely difficult to accurately analyse on a 100% aqueous mobile phase.

Differential scanning fluorimetry (DFS)
Thermal protein stability in response to compound binding was assessed as a qualitative measure of the ability of the protein to bind and is expressed as temperature shift (ΔT_m). DDB1-CRBN or DDB1-CRBN(YW/AA) mutant complex (50 µg/ml), 5x Sypro Orange, 2% final DMSO and corresponding amounts of compound were mixed in assay buffer (50 mM HEPES pH 7.5, 200 mM NaCl, 0.2 mM TCEP). Samples were heated while measuring the association of Sypro Orange with hydrophobic groups upon protein unfolding. Wild type and mutant CRBN showed comparable behaviour with inflection points (ΔT_m(inf)) of 56.2°C and 55.4°C, respectively. The dose-responses of compounds were tested with serial dilutions of 200-0.6 nM.

Ubiquitin ligase substrate profiling by protein microarray

On-chip ubiquitination assay: Human ProtoArray microarrays were equilibrated at 4°C for 10 min and blocked for 2 h at 4°C with blocking buffer (50 mM HEPES pH 7.4, 200 mM NaCl, 0.08% Triton-X 100, 25% glycerol, 20 mM glutathione, 1 mM DTT, 1% protease-free BSA adjusted to a pH of 7.5-8.0). Blocking buffer was removed and the arrays washed for 5 min at 4°C with 5 ml of assay buffer (50 mM

HEPES pH 7.4, 50 mM NaCl, 5 mM $MgSO_4$, 0.1% Tween 20, 1% BSA, and 1 mM DTT). Ubiquitin ligase mixtures were prepared in assay buffer containing 100 nM E1 (Uba1), 1,000 nM E2 (UbcH5A), 500 nM E3 ($CRL4A^{CRBN}$ or control $CRL4A^{CDT2}$), 10 µM biotin-ubiquitin and 1 mM ATP and if appropriate 200 nM CSN_{ASM} or 50 µM lenalidomide in a final volume of 170 µl. Under the assumption that CRLs are fast and processive enzymes[17], relative complete inactivation of the $CRL4^{CRBN}$ ligase is required to achieve a significant signal under *in vitro* conditions. With a K_d for CRBN of 177.8 nM, a relatively high concentration of lenalidomide would be required to largely inhibit ligase activity. Similar requirements for high inhibitor concentrations were also observed in subsequent cellular and *in vitro* assays. The ligase mixture was pre-incubated for 5 min at 30°C before addition of ATP and distributed evenly on the array surface immediately after ATP addition. The arrays were covered with Lifterslips (Thermo Scientific) and incubated for 90 min at room temperature. Assay buffer (5 ml) was added to carefully remove the Lifterslips and the arrays washed 3 times for 5 min with 0.5% SDS (in 50 mM Tris-HCl pH 8.0) solution, followed by 3 washes (5 min) with assay buffer, and were finally probed with Alexa647-Streptavidin (1 µg/ml) for 45 min. The Alexa647-Streptavidin solution was removed and the arrays washed 4 times with assay buffer, followed by a wash in ddH_2O (5 min) and drying by centrifugation.

Image acquisition and processing: Slides were scanned using a GenePix 4200A (Molecular Devices) and images quantified using GenePix Pro 5 feature extraction software (Molecular Devices). Scanning parameters were set to PMT gain value = 450 to avoid spot oversaturation.

Data processing and normalisation: Protein arrays were normalised using the "limma" Bioconductor package[18] as follows: median estimates for foreground and background intensities were imported from raw data files. Arrays were corrected using background values derived from the minimum of the backgrounds of each spot and its eight neighbours (method "movingmin" of the "backgroundCorrect" function). A small fraction of the background-corrected intensities were negative (between 0.2% and 8% of values on each array, total data ranging from -32 to 65480). To render all background-corrected intensities greater than 0, the minimum intensity minus one (-33) was subtracted and the resulting intensities log2 transformed. Reproducibility of replicates was assessed, excluding spots marked by "Control" or "Internal Control" in the array annotation, by calculating Pearson correlation coefficients of log intensities between pairs of arrays. Correlation coefficients over any pair of arrays ranged from 0.76 to 0.97 (within replicate groups from 0.94 to 0.97). Log2 intensities were then quantile normalised.

By definition, a specific target of $CRL4^{CRBN}$ is expected to have a very low intensity on negative control arrays E1+E2, low intensity on arrays incubated with an alternative E3 ligase ($CRL4^{CDT2}$) or with $CRL4^{CRBN}$ in the presence of inhibitors ($CRL4^{CRBN}$+Lenalidomide), and high intensity on arrays with $CRL4^{CRBN}$ or CRBN in the presence of CSN ($CRL4^{CRBN}$+CSN). The intensities (I) of a specific CRBN target

should increase over arrays in the order: I(E1+E2) = I($CRL4^{CDT2}$) < I($CRL4^{CRBN}$+Lenalidomide) < I($CRL4^{CRBN}$+CSN) < I($CRL4^{CRBN}$). To identify proteins that agree with these criteria, we performed cluster analysis using the "clara" partitioning method from the package "cluster" in R[19]. Replicate spots on each array, and then replicate arrays were averaged, control spots were removed, and the values for each protein scaled to mean 0 and unit variance across conditions. The optimal number of clusters (k=43) was chosen by varying the number between 20 and 100 and selecting the one with the highest average silhouette width (a comparison of intra- and inter-cluster distances). Clusters with intensity profiles similar to the expected profile for specific targets were selected manually.

Cell culture and western blot analysis

HEK293T and M059J cells were grown in DMEM supplemented with 10% FBS and 2 mM L-glutamine. SK-N-DZ cells were grown in DMEM supplemented with 10% FBS, 2 mM L-glutamine, and 1x non-essential amino acids (NEAA). For knockdown experiments, 10 pmol siRNA specific to the target gene (sequences: GACAUUACCUCUUCAGCUU, GUAUAAGGCUUGCAACUUG, CGACUUCGCUGUGAAUUAG, CAAUUAGAAUCCCUCAAUA) was transfected using the RNAiMAX (Invitrogen) transfection reaction according to the manufacturer's instructions and incubated for 48-72 h. For compound treatment, cells were grown to approximately 80% confluence and the medium exchanged for growth medium containing the desired compound or equivalent amounts of DMSO as control. Cells were incubated for varying times as indicated. For overexpression of MEIS2, DDK epitope-tagged MEIS2 ORFs were purchased from Origene and transiently transfected using X-tremeGene 9 (Roche) according to the manufacturer's instructions. Cells were grown for 48 h prior to compound treatment. Cycloheximide chase experiments were performed by pretreating cells with the indicated compounds for 30 min and subsequent addition of cycloheximide from a 20 mg/ml stock solution. For western blot analysis, cells were lysed directly in 24-well plates by addition of 100 to 200 µl 1x LDS sample buffer (NuPAGE 4x LDS sample buffer) supplemented with a reducing agent, heated at 90°C for 10 min and subjected to SDS-PAGE and subsequent western blotting. Benzonase 0.5 µl/well was added to solubilise lysates. Protein levels were monitored using DDK or antigene-specific primary antibodies and infrared fluorophor conjugated secondary antibodies.

RT-qPCR assay: Measurement of Meis2 transcript levels in the human HEK293 cell line by quantitative reverse transcription PCR (RT-qPCR) was perfomed using the UPL (Universal Probe library) assay from Roche (FwdPrimer: GCAAAGCAAGGGGGAAGT; RevPrimer: GTCATCTGGGGAGGAGTGTAA; ProbeID: MEIS2.1 and FwdPrimer: GACAAGGACGCGATCTATGG; RevPrimer: TCGCACTTCTCAAAGACCAG; ProbeID: MEIS2.2). Cells were washed once with PBS at room temperature before addition of 15 µL per sample of Roche lysis buffer

containing a 1:80 dilution of RNAse inhibitor. Samples were incubated for 10 minutes at room temperature and stored at 4 °C until further processing. Reverse transcription was performed using RT kit components from Life Technologies. In short, 3 µl lysate were added to 17 µl RT mix consisting of 10 µl 2x RT buffer, 1 µl 20x RT Enzyme mix and 6 µl Water. Samples were incubated for 60min at 37 °C followed by 5min at 95 °C to stop the reaction. qPCR reactions were performed according to the vendors recommendations. cDNA (2ul RT reaction) was added to 8 µl qPCR mix consisting of 5 µl Taqman master mix 2x (Life Technologies), 0.5 µl Actin assay 20x (Roche), 0.25 µl UPL probe (Roche), 0.9 µl primer mix (10 µM) and 1.35 µl water. Cycling was performed on a ViiA7 qPCR instrument (Life Technologies) using FAST cycling conditions:

Cycles	**Temperature**	**Hold time**
1	95 °C	20s
40	95 °C	1s
	60 °C	20s

Ct values were called using automatic baseline and threshold settings from the ViiA7 software. DeltaCt values for target minus housekeeper were calculated per well inside of Spotfire software. Calculation of DeltaDeltaCt values was based on the median DeltaCt values for DMSO treated control wells. Corresponding RQ (relative quantity) values were calculated using 2-DeltaDeltaCt.

Luciferase Ikaros degradation assay: A plasmid encoding firefly luciferase (Fluc) Ikaros fusion protein and renilla luciferase (Rluc) protein was a kind gift from W. Kaelin and experiments were performed as described by Lu and colleagues[14]. In brief, HEK293T cells grown in 96-well plates were transfected with 20 ng/well of plasmid using FugeneHD transfection reagent. Following a 24-h incubation, appropriate amounts of DMEM containing different compounds or DMSO were added to the wells to reach the desired final concentrations and the cells incubated for a further 12 h. Luciferase detection was carried out using the Dual-Glo kit (Promega) according to the manufacturer's instructions and the luminescence signal was acquired on a Gemini multimode plate reader (Molecular Devices).

Zebrafish experiments: Embryos for the zebrafish experiments were obtained from natural spawning of the AB strain and maintained in E3 embryo media at 28.5°C as previously described[20]. Thalidomide was added 2 h post-fertilisation (hpf) from a 100 mM stock solution in DMSO to yield final concentrations of 0.4, 0.7 and 1.0 mM thalidomide. Lysates for western blots were prepared by collecting 10 embryos at the 24 hpf in a 1.5-ml microcentrifuge tube, removing excess buffer, adding 40 µl of 4X NuPAGE LDS Sample Buffer (Novex), 10 µl 10X NuPAGE Sample Reducing Agent (Novex), and water to 100 µl, manually macerating the tissue using a pestle and immediately heating the sample to 100°C. One embryo equivalent (10 µl) of each sample was analysed by western blotting using anti-MEIS2 (Abnova) and anti-GAPDH (Sigma) antibodies.

Mapping of ubiquitin and phosphorylation sites by LC-MS/MS: The $CRL4A^{CRBN}$ complex and MEIS2 were subjected to *in vitro* ubiquitination and subsequently analysed by LC-MS/MS as described earlier for DDB2[25]. Alternatively, trichloroacetic acid-precipitated and acetone-washed proteins were digested with 200 ng endoproteinase Lys-C for 6 h at 37°C, followed by 200 ng trypsin overnight at 37°C. Generated peptides were separated on an EASY n-LC 1000 liquid chromatography system equipped with a 75 µm x 15 cm PepMap C18 EASY-Spray column coupled to an LTQ Orbitrap Velos mass spectrometer (all from Thermo Scientific). The ubiquitinated or phosphorylated peptides were identified with Mascot searching Swiss-Prot 2012_09 (Matrix Science) and validated with ScaffoldPTM (Proteome Software). Quantitative analysis was done with ProgenesisLC (Nonlinear Dynamics).

Procedures for chemical synthesis, purification and analyses of thalidomide derivatives

General: All solvents employed were commercially available "anhydrous" grade and reagents were used as received unless otherwise noted. Cy5 *N*-hydroxysuccinimide (NHS) ester was purchased from Lumiprobe. Flash column chromatography was performed on an Analogix Intelliflash 280 using Si 50 columns (32-63 µm, 230-400 mesh, 60 Å) or on a Biotage SP1 system (32-63 µm particle size, KP-Sil, 60 Å pore size). Preparative high pressure liquid chromatography (HPLC) was performed using a Waters 2525 pump with a 2487 dual wavelength detector and a 2767 sample manager. Columns used were Waters C18 OBD 5 µm, either 50 × 100 mm Xbridge or 30 × 100 mm Sunfire. NMR spectra were recorded on a Bruker AV400 (Avance 400 MHz) instrument. Analytical LC-MS was conducted using an Agilent 1100 with UV detection at 214 and 254 nm and an electrospray mode (ESI) coupled with a Waters ZQ single quad mass detector.

1) Preparation of *N*-(4-aminobutyl)-2-((2-(2,6-dioxopiperidin-3-yl)-1,3-dioxoisoindolin-4-yl)oxy)acetamide (4):

a) *tert*-Butyl (4-(2-chloroacetamido)butyl)carbamate:

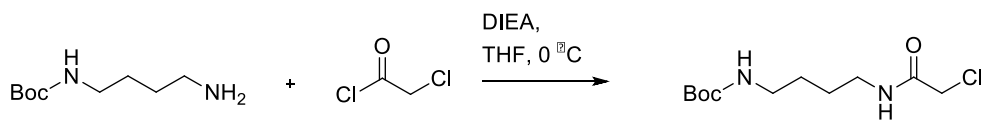

2-Chloroacetyl chloride (0.189 mL, 2.34 mmol) followed by DIEA (0.371 mL, 2.13 mmol) were added to a solution of *tert*-butyl (4-aminobutyl)carbamate (0.407 mL, 2.12 mmol) in THF (21 mL) at 0°C. The resulting solution was allowed to warm to room temperature over 3 h. The reaction was then diluted with EtOAc (50 mL) and water (50 mL). The organic layer was separated, washed with water (2 x 20 mL), dried (Na_2SO_4) and concentrated. The crude product was used in the next step without further purification.

b) 3-((4(*N*-Boc-aminobutyl)amino)-2-oxoethoxy)-phthalic acid dimethyl ester:

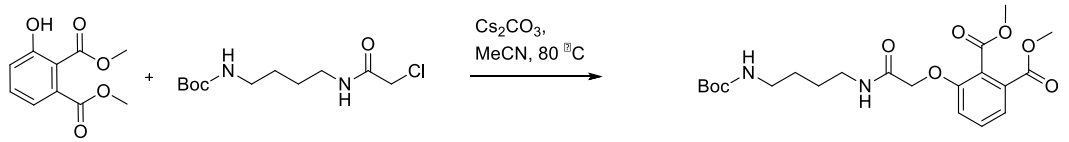

A solution of 3-hydroxyphthalic acid dimethyl ester (500 mg, 2.38 mmol) in MeCN (13 mL) was treated with the crude *tert*-butyl (4-(2-chloroacetamido)butyl)carbamate (2.12 mmol) and Cs_2CO_3 (1.9 g, 5.82 mmol). The resulting mixture was heated at 80°C for 12 h and then concentrated under reduced pressure. The reaction was then diluted with EtOAc (50 mL) and water (20 mL). The organic layer was separated, washed with water (2 x 20 mL), dried (Na_2SO_4) and concentrated. The crude product was purified by silica gel chromatography eluting with 0-20% MeOH:DCM to afford the title compound (650 mg, 70% yield, two steps). ^{1}H NMR (CHLOROFORM-*d*) δ ppm 7.58 (d, *J*=7.8 Hz, 1 H), 7.42 (app. t, *J*=8.2 Hz, 1 H), 7.10 (d, *J*=7.8 Hz, 1 H), 7.02 (br.s, 1H), 4.73 (br.s, 1 H), 4.54 (s, 2 H), 3.90 (s, 3 H), 3.85 (s, 3 H), 3.26 (q, *J*=6.8 Hz, 2 H), 3.06 (q, *J*=6.4 Hz, 2 H), 1.51 (m, 2 H), 1.43 (m, 2 H), 1.37 (s, 9 H); ^{13}C NMR (CHLOROFORM-*d*) δ ppm 26.4, 27.0, 28.2, 38.6, 39.9, 52.6, 52.8, 67.9, 78.8, 116.8, 123.1, 124.6, 129.7, 130.9, 154.2, 155.8, 165.5, 167.3, 167.9; MS *m/z* 439.3 (MH^+).

3-((4(*N*-Boc-aminobutyl)amino)-2-oxoethoxy)-phthalic acid[21]

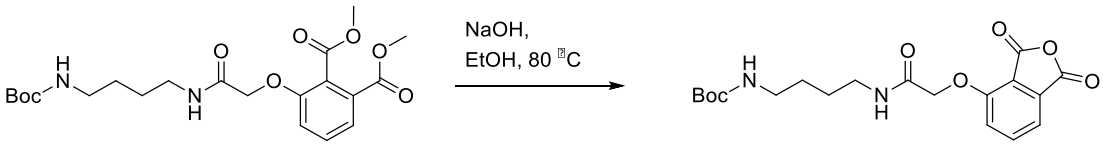

3N NaOH (1.5 mL, 4.50 mmol) was added to a solution of 3-((4-(*N*-Boc-aminobutyl)amino)-2-oxoethoxy)-phthalic acid dimethyl ester (650 mg, 1.48 mmol) in EtOH (15 mL) and the resulting mixture heated at 80°C for 2 h. The reaction was concentrated under reduced pressure and the crude mixture dissolved in water (50 mL) and CH_2Cl_2 (50 mL) and then acidified using 1N HCl. The organic layer was separated, washed with water (2 x 20 mL), dried ($MgSO_4$) and concentrated under reduced pressure. The crude product was used in the next step without further purification.

***N*-(4-Aminobutyl)-2-((2-(2,6-dioxopiperidin-3-yl)-1,3-dioxoisoindolin-4-yl)oxy)acetamide (4):**

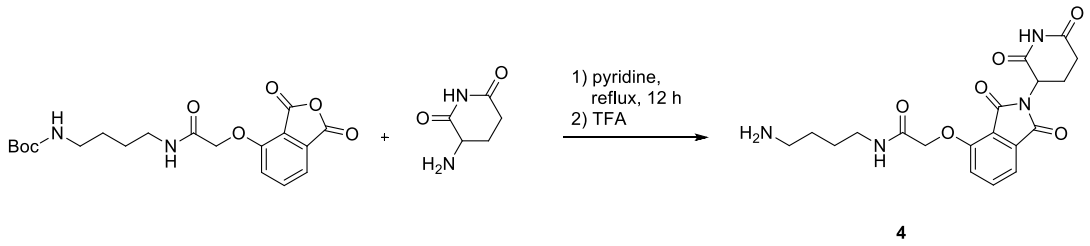

4

3-Aminopiperidine-2,6-dione (105 mg, 0.637 mmol) was added to a solution of 3-((4(*N*-Boc-aminobutyl)amino)-2-oxoethoxy)-phthalic acid (250 mg, 0.637 mmol) in pyridine (6.4 mL) and the resulting solution heated with reflux for 12 h. On cooling, the reaction was concentrated under reduced pressure and the crude product purified by prep-HPLC eluting with 10-90% MeCN:water and 0.1% TFA. The desired Boc-protected product was isolated, dissolved in DCM (2 mL) and treated with TFA (2 mL) at 50°C for 2 h. Purification by prep-HPLC eluting with 10-90% MeCN:water and 0.1% TFA afforded the desired product as a white solid (60 mg, 23% yield). ^{1}H NMR (METHANOL-d_4) d ppm 7.82 (dd, *J*=7.8 Hz, 1 H), 7.53 (d, *J*=7.3 Hz, 1 H), 7.45 (d, *J*=8.5 Hz, 1 H), 5.15 (dd, *J*=12.5, 5.3 Hz, 1 H), 4.79 (s, 2 H), 3.36 (m, 2 H), 2.97 (m, 2 H), 2.89 (m, 1 H), 2.73 (m, 2 H), 2.16 (m, 1 H), 1.69 (m, 4 H); ^{13}C NMR (METHANOL-d_4) d ppm 23.8, 25.9, 27.4, 32.3, 39.5, 40.5, 50.6, 69.6, 118.2, 119.4, 122.1, 134.9, 138.5, 156.4, 168.0, 168.4, 170.3, 171.6, 174.7; HRMS (ESI-TOF) *m/z* calculated for $C_{19}H_{22}N_4O_6$ (MH^+) 403.1618, found 403.1621.

2) Preparation of thalidomide-Cy5 conjugate (5):

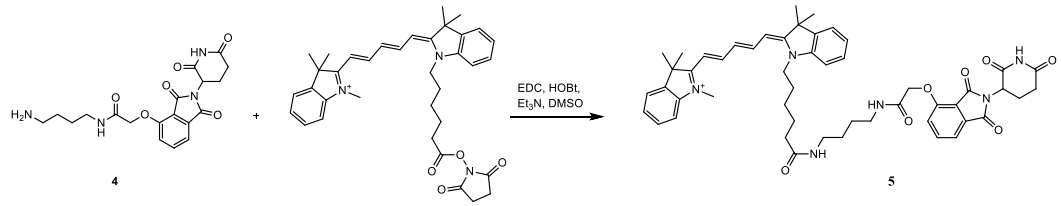

4 5

A solution of **4** (4.5 mg, 20.25 µmol) in DMSO (0.5 mL) was added to a solution of Cy5-NHS ester (5 mg, 8.11 µmol) and Et_3N (2.25 µL, 0.016 mmol) in DMSO (0.5 mL) at ambient temperature. The reaction mixture was stirred for 2 h prior to addition of EDC (1.8 mg, 9.7 µmol), HOBT (1.2 mg, 8.1 µmol) and Et_3N (2.3 µL, 0.016 mmol). The resulting mixture was stirred for 12 h before being filtered through a glass pipette containing Si-carbonate (50 mg, SiliCycle 0.55 mmol/g), eluting with MeOH. Purification by prep-HPLC eluting with 21-60% MeCN:water and 0.1% TFA afforded the title compound **5** as a deep-blue powder (3.7 mg, 45% yield). ^{1}H NMR (DMSO-d_6) δ ppm 11.11 (s, 1H), 8.32 (t, *J*=13.1 Hz, 2H), 7.95 (t, *J*=5.8 Hz, 1H), 7.77-7.85 (m, 1H), 7.73 (t, *J*=5.6 Hz, 1H), 7.61 (d, *J*=7.6 Hz, 2H), 7.49 (d, *J*=7.6 Hz, 1H), 7.34-7.44 (m, 5H), 7.24 (dd, *J*=13.4, 7.8 Hz, 2H), 6.55 (t, *J*=12.6 Hz, 1H), 6.27 (dd, *J*=19.2, 14.1 Hz, 2H), 5.11 (dd, *J*=12.6, 5.6 Hz, 1H), 4.75 (s, 2H), 4.07 (t, *J*=6.6 Hz, 2H), 3.13 (q, *J*=6.2 Hz, 3H), 3.00 (q, *J*=5.7 Hz, 2H), 2.04 (t, *J*=7.1 Hz, 3H), 1.68

(s, 15H), 1.47-1.58 (m, 3H), 1.28-1.45 (m, 7H); MS *m/z* 867.4 (M+); Purity by analytical LC/MS (Inertsil 150 × 4.6 mm C18 column used at a flow rate of 1.2 mL/min with a gradient of 10-95% acetonitrile/water and 0.1% TFA over 15 min): T_r= 6.51 min and >95% purity at 254 and 214 nm.

3) Preparation of 2-(2,6-dioxopiperidin-3-yl)4-methylisoindolin-1,3-dione (6):

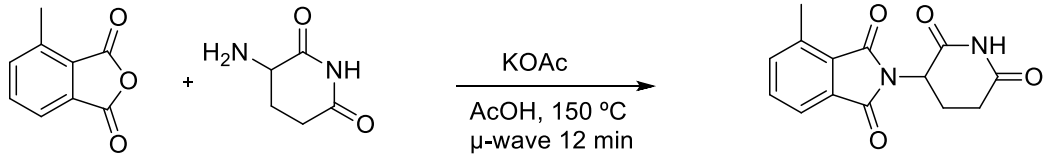

6

Acetic acid (3 mL) was added to 3-methylphthalic anhydride (52 mg, 0.306 mmol), 3-aminopiperidine-2,6-dione (55 mg, 0.334 mmol) and KOAc (74 mg, 0.754 mmol). The reaction mixture was heated in a microwave at 150 °C for 12 min, allowed to cool and then diluted with water and filtered. The solid was washed with water (x2) then saturated aqueous $NaHCO_3$ solution. The solid was then washed with water followed by diethyl ether (x5) prior to drying under vacuum filtration for 10 min. The crude product was treated with methanol:water (1:1) and the resultant suspension was filtered and washed with methanol:water (1:1), followed by diethyl ether prior to drying to give a white solid (40 mg, 47% yield). ^{1}H NMR (DMSO-d_6) d ppm 11.12 (br. s, 1 H), 7.79-7.72 (m , 2 H), 7.71-7.65 (m, 1 H), 5.13 (dd, *J*=12.9, 5.3 Hz, 1 H), 2.97-2.81 (m, 1 H) 2.60-2.45 (m, 4 H), 2.12-1.99 (m, 1 H); ^{13}C NMR (DMSO-d_6) d ppm 17.1, 22.0, 31.0, 48.8, 121.1, 127.9, 131.7, 134.4, 137.0, 137.6, 167.1, 167.9, 170.0, 172.9; MS *m/z* 273.1 (M+H); HRMS (ESI-TOF) *m/z* calculated for $C_{14}H_{13}N_2O_4$ (MH^+) 273.0870, found 273.0894. Purity by analytical LC/MS (Acquity UPLC BEH 50 × 2.1 mm C18 column used at a flow rate of 1.0 mL/min with a gradient of 1-99% acetonitrile/water and 0.1% formic acid over 8.05 min): T_r= 3.28 min and >98% purity at 254 and 214 nm.

4) Preparation of 4-chloro-2-(2,6-dioxopiperidin-3-yl)isoindolin-1,3-dione (7):

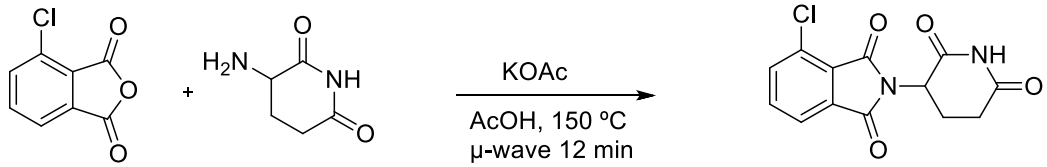

7

Acetic acid (3 mL) was added to 4-chloroisobenzofuran-1,3-dione (87 mg, 0.477 mmol), 3-aminopiperidine-2,6-dione (88 mg, 0.532 mmol) and KOAc (98 mg, 1.001 mmol). The reaction mixture was heated in a microwave at 150 °C for 12 min, allowed to cool and then diluted with water and filtered. The solid was washed with water (x2) then saturated aqueous $NaHCO_3$ solution. The solid was then washed with

water followed by diethyl ether (x5) prior to drying under vacuum filtration for 10 min. The crude product was dried to give a the target compound (116 mg, 79% yield). ^{1}H NMR (DMSO-d_6) d ppm 11.15 (s, 1 H), 8.14-7.62 (m , 3 H), 5.17 (dd, *J*=12.9, 5.3 Hz, 1 H), 2.99-2.81 (m, 1 H) 2.68-2.52 (m, 2 H), 2.17-2.02 (m, 1H); ^{13}C NMR (DMSO-d_6) d ppm 21.8, 30.9, 49.1, 122.4, 126.9, 129.8, 133.5, 136.1, 136.4, 164.8, 165.7, 169.7, 172.7; MS *m/z* 292.7 (M+H); HRMS (ESI-TOF) *m/z* calculated for $C_{13}H_{10}ClN_2O_4$ (MH^+) 293.0329, found 293.0305. Purity by analytical LC/MS (Acquity UPLC BEH 50 × 2.1 mm C18 column used at a flow rate of 1.0 mL/min with a gradient of 2-99% acetonitrile/water and 0.1% formic acid over 8.05 min): T_r= 2.98 min and >98% purity at 254 and 214 nm.

5) Preparation of 2-(2,6-dioxopiperidin-3-yl)-5-methylisoindolin-1,3-dione (8):

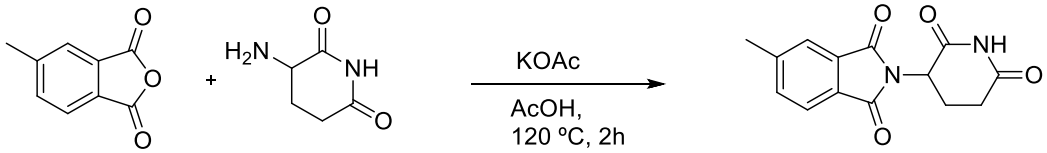

8

Acetic acid (3 mL) was added to 4-methylphthallic anhydride (64 mg, 0.375 mmol), 3-aminopiperidine-2,6-dione (68 mg, 0.413 mmol) and KOAc (114 mg, 1.162 mmol). The reaction mixture was heated at 120 °C for 2 h, allowed to cool and then diluted with water and filtered. The solid was washed with water (x2) then saturated aqueous $NaHCO_3$ solution (x3). The solid was then washed with water followed by diethyl ether (x5) prior to drying under vacuum filtration for 10 min. The crude product was dried to give the target compound (77 mg, 75% yield). ^{1}H NMR (DMSO-d_6) d ppm 11.14 (s, 1 H), 7.82 (d, *J*=7.8 Hz, 1 H), 7.77 (s, 1 H), 7.70 (d, *J*=7.5 Hz, 1 H), 5.14 (dd, *J*=12.8, 5.3 Hz, 1 H), 2.97-2.83 (m, 1 H), 2.65-2.53 (m, 2 H), 2.50 (s, 3 H), 2.11-2.00 (m, 1H); ^{13}C NMR (DMSO-d_6) d ppm 21.4, 22.1, 31.0, 48.9, 123.4, 123.9, 128.7, 131.6, 135.2, 146.0, 167.2, 170.0, 172.8; MS *m/z* 273.1 (M+H); HRMS (ESI-TOF) *m/z* calculated for $C_{14}H_{13}N_2O_4$ (MH^+) 273.0875, found 273.0881. Purity by analytical LC/MS (Acquity UPLC BEH 50 × 2.1 mm C18 column used at a flow rate of 1.0 mL/min with a gradient of 1-99% acetonitrile/water and 0.1% formic acid over 8.05 min): T_r= 3.21 min and >98% purity at 254 and 214 nm.

6) Preparation of 2-(2,6-dioxopiperidin-3-yl)-4,6-dimethylisoindolin-1,3-dione (9):

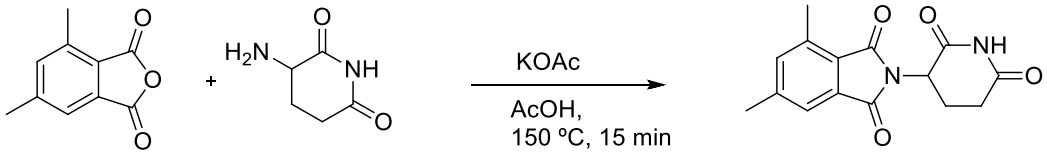

9

Acetic acid (3 mL) was added to 4,6-dimethylisobenzofuran-1,3-dione (55 mg, 0.312 mmol), 3-aminopiperidine-2,6-dione (62 mg, 0.377 mmol) and KOAc (74 mg, 0.754 mmol). The reaction mixture was heated in a microwave at 150 °C for 15 min, allowed to cool and then diluted with ethyl acetate and filtered. The mixture was washed with ethyl acetate (x7) and the resultant white solid dried under vacuum yielding the target compound (52 mg, 57% yield). ^{1}H NMR (DMSO-d_6) d ppm 11.13 (br. s, 1 H), 7.57 (s, 1 H), 7.49 (s, 1 H), 5.11 (dd, *J*=12.7, 4.9 Hz, 1 H), 2.98-2.80 (m, 1 H), 2.65-2.55 (m, 5 H), 2.45 (s, 3 H), 2.10-1.98 (m, 1 H); ^{13}C NMR (DMSO-d_6) d ppm 17.0, 21.2, 22.1, 31.0, 48.7, 121.7, 125.4, 132.0, 137.2, 137.4, 145.3, 167.2, 167.8, 170.0, 172.9; MS *m/z* 287.1 (M+H); HRMS (ESI-TOF) *m/z* calculated for $C_{15}H_{15}N_2O_4$ (MH^+) 287.1032, found 287.1040. Purity by analytical LC/MS (Acquity UPLC BEH 50 × 2.1 mm C18 column used at a flow rate of 1.0 mL/min with a gradient of 1-99% acetonitrile/water and 0.1% formic acid over 8.05 min): T_r= 4.22 min and >98% purity at 254 and 214 nm

Supplementary Discussion

A structural and mechanistic view of thalidomide teratogenicity

Thalidomide, lenalidomide and pomalidomide display differential anti-proliferative efficacy in multiple myeloma therapy, which has been attributed to their varying abilities to induce Ikaros/Aiolos degradation when bound to CRBN[22-24]. Yet, thalidomide, lenalidomide and pomalidomide have similar teratogenic properties[25,26], which appear unrelated to Ikaros/Aiolos degradation. Our findings suggest two possible mechanisms that explain how IMiDs induce teratogenicity: (*i*) by increasing the cellular concentration of an endogenous substrate, blocking its binding to the receptor; and (*ii*) by degrading a *neo*-substrate in response to IMiD treatment. The two options are not necessarily mutually exclusive, and could also function in a synthetic manner. When bound by CRBN, the solvent-exposed face of thalidomide, lenalidomide and pomalidomide (C4-C5-C6) is small and only 1 of the 3 positions differs in thalidomide compared with lenalidomide and pomalidomide. Modifying a single C4-C5-C6 substituent thus is a relatively large change. This makes it unlikely that a *neo*-substrate exists that can be equally recruited by the three compounds and elicit equal teratogenic effects. All glutarimide-containing IMiDs bind to the

canonical CRBN substrate interface through a shared pharmacophore; and all IMiDs accordingly counteract binding of endogenous substrates to a comparable extent, as exemplified by MEIS2. We favour a model where an endogenous substrate, either MEIS2 or another protein, acts as the embryotoxic trigger. This is supported by findings that some of the pleiotropic effects of thalidomide can be uncoupled[27] by changes of surface-exposed moieties, while retaining teratogenicity.

MEIS2: a candidate for aspects of thalidomide-induced teratogenicity

The precise identity of the substrate that induces teratogenicity remains unclear at present. CRL ligases commonly have multiple endogenous substrates[28-31] and it is plausible that multiple substrates of the $CRL4^{CRBN}$ ligase exist. Any of these, or a combination thereof, could be responsible for the phenotype. Clinically, the CRBN receptor is implicated in a range of disease manifestations ranging from mental retardation to thalidomide-mediated immune-modulatory and anti-cancer properties. It is unlikely that all this clinical manifestations are linked to IMiD mediated Ikaros degradation.

In this study, we identify MEIS2 as an endogenous CRBN substrate. MEIS2 is a transcription factor implicated in many aspects of normal human development. Mutations in human MEIS2 cause mental retardation[32], cleft palate[33,34], and in animal models have been linked to problems in lens and retina development and congenital cardiac defects[35,36]. Ectopic MEIS2 overexpression across the whole limb bud induces digit tip truncations in chicken embryos[37].

Thalidomide syndrome, owing to thalidomide exposure during pregnancy (weeks 3-6), is characterized by pleiotropic malformations of a multitude of organs, which amongst others also include the limbs, face, heart and other internal organs. Many unborn babies exposed to thalidomide died *in utero* owing to widespread organ malformation. The organs whose development is influenced by MEIS2 and those affected by thalidomide exposure show some overlap, however, the detailed clinical phenotypes caused by MEIS2 mutations/localised overexpression differ from those seen in patients following thalidomide exposure *in utero* (for example digit tip truncation in ectopic MEIS2 overexpression is rare in thalidomide syndrome). Following thalidomide exposure, the steady state levels of MEIS2 are increased ~2-fold. It is notable that a 2-fold change in a related transcription factor, Pax6 haploinsufficiency for an example[38], results in significant developmental phenotypes. While a developmental transcription factor such as MEIS2 that interplays with HOX genes could be implicated in the pleiotropic malformations seen following thalidomide exposure, there are currently no data that allow the two to be directly linked.

Supplementary references

1 Abdulrahman, W. *et al.* A set of baculovirus transfer vectors for screening of affinity tags and parallel expression strategies. *Anal Biochem* **385**, 383-385, (2009).

2 Kabsch, W. Automatic Processing of Rotation Diffraction Data from Crystals of Initially Unknown Symmetry and Cell Constants. *Journal of Applied Crystallography* **26**, 795-800 (1993).
3 Winn, M. D. *et al.* Overview of the CCP4 suite and current developments. *Acta crystallographica. Section D, Biological crystallography* **67**, 235-242, (2011).
4 Mccoy, A. *et al.* Phaser crystallographic software. *Journal of Applied Crystallography* **40**, 658-674 (2007).
5 Vagin, A. & Teplyakov, A. MOLREP: an automated program for molecular replacement. *Journal of Applied Crystallography* (1997).
6 Adams, P. D. *et al.* PHENIX: a comprehensive Python-based system for macromolecular structure solution. *Acta Crystallographica Section D-Biological Crystallography* **66**, 213-221, (2010).
7 Emsley, P. & Cowtan, K. Coot: model-building tools for molecular graphics. *Acta Crystallographica Section D-Biological Crystallography* **60**, 2126-2132 (2004).
8 Bricogne, G. *et al.* BUSTER version 2.9. *Cambridge, United Kingdom: Global Phasing Ltd.* (2010).
9 Allen, F. H. The Cambridge Structural Database: a quarter of a million crystal structures and rising. *Acta Crystallogr B* **58**, 380-388 (2002).
10 Davis, I. W. *et al.* MolProbity: all-atom contacts and structure validation for proteins and nucleic acids. *Nucleic acids research* **35**, W375-383, (2007).
11 Duda, D. *et al.* Structural insights into NEDD8 activation of cullin-RING ligases: conformational control of conjugation. *Cell* **134**, 995-1006, (2008).
12 Fischer, E. S. *et al.* The Molecular Basis of CRL4DDB2/CSA Ubiquitin Ligase Architecture, Targeting, and Activation. *Cell* **147**, 1024-1039, (2011).
13 Sugasawa, K. The xeroderma pigmentosum group C protein complex and ultraviolet-damaged DNA-binding protein: functional assays for damage recognition factors involved in global genome repair. *Methods Enzymol* **408**, 171-188, (2006).
14 Marks, B. D. *et al.* Multiparameter analysis of a screen for progesterone receptor ligands: comparing fluorescence lifetime and fluorescence polarization measurements. *Assay and Drug Development Technologies* **3**, 613-622, (2005).
15 Nikolovska-Coleska, Z. *et al.* Development and optimization of a binding assay for the XIAP BIR3 domain using fluorescence polarization. *Anal Biochem* **332**, 261-273, (2004).
16 Valko, K., Du, C. M., Bevan, C. D., Reynolds, D. P. & Abraham, M. H. Rapid-gradient HPLC method for measuring drug interactions with immobilized artificial membrane: comparison with other lipophilicity measures. *Journal of pharmaceutical sciences* **89**, 1085-1096 (2000).
17 Pierce, N. W., Kleiger, G., Shan, S.-O. & Deshaies, R. J. Detection of sequential polyubiquitylation on a millisecond timescale. *Nature* **462**, 615-619, (2009).
18 Smyth, G. K. *Limma: linear models for microarray data*. 397-420 (Springer, 2005).
19 Maechler, M. R., P; Struyf, A; Hubert, M; Hornik, K. cluster: Cluster Analysis Basics and Extensions. R package version 1.14.4. (2013).
20 Nuesslein-Volhard, C. & Dahm, R. *Zebrafish*. (Oxford University Press, 2002).
21 Ruchelman, A. L. 4'-0-substituted isoindole derivatives and compositions comprising and methods of using the same. USA patent (2008).
22 Gandhi, A. K. *et al.* Immunomodulatory agents lenalidomide and pomalidomide co-stimulate T cells by inducing degradation of T cell repressors Ikaros and Aiolos via modulation of the E3 ubiquitin ligase complex CRL4(CRBN.). *British journal of haematology* **164**, 811-821, (2014).
23 Lu, G. *et al.* The myeloma drug lenalidomide promotes the cereblon-dependent destruction of Ikaros proteins. *Science* **343**, 305-309, (2014).

24 Kronke, J. *et al.* Lenalidomide causes selective degradation of IKZF1 and IKZF3 in multiple myeloma cells. *Science* **343**, 301-305, (2014).
25 Heger, W. *et al.* Embryotoxic effects of thalidomide derivatives on the non-human primate Callithrix jacchus; 3. Teratogenic potency of the EM 12 enantiomers. *Archives of toxicology* **62**, 205-208 (1988).
26 Smith, R. L., Fabro, S., Schumacher, H. & Williams. in *Embryopathic Activity of Drugs, Biological Council Symposium* (eds J.M. Robson, F. Sullivan, & R.L. Smith) 194-209 (Churchill, 1965).
27 Dredge, K. *et al.* Novel thalidomide analogues display anti-angiogenic activity independently of immunomodulatory effects. *British journal of cancer* **87**, 1166-1172, (2002).
28 Skaar, J. R., Pagan, J. K. & Pagano, M. Mechanisms and function of substrate recruitment by F-box proteins. *Nat Rev Mol Cell Biol* **14**, 369-381, (2013).
29 Lee, J. & Zhou, P. Pathogenic Role of the CRL4 Ubiquitin Ligase in Human Disease. *Frontiers in oncology* **2**, 21, (2012).
30 Scrima, A. *et al.* Detecting UV-lesions in the genome: The modular CRL4 ubiquitin ligase does it best! *FEBS letters*, (2011).
31 Bennett, E. J., Rush, J., Gygi, S. P. & Harper, J. W. Dynamics of Cullin-RING Ubiquitin Ligase Network Revealed by Systematic Quantitative Proteomics. *Cell* **143**, 951-965, (2010).
32 Johansson, S. *et al.* Haploinsufficiency of MEIS2 is associated with orofacial clefting and learning disability. *Am J Med Genet A*, (2014).
33 Crowley, M. A. *et al.* Further evidence for the possible role of MEIS2 in the development of cleft palate and cardiac septum. *Am J Med Genet A* **152A**, 1326-1327, (2010).
34 Erdogan, F. *et al.* Characterization of a 5.3 Mb deletion in 15q14 by comparative genomic hybridization using a whole genome "tiling path" BAC array in a girl with heart defect, cleft palate, and developmental delay. *Am J Med Genet A* **143**, 172-178, (2007).
35 Paige, S. L. *et al.* A temporal chromatin signature in human embryonic stem cells identifies regulators of cardiac development. *Cell* **151**, 221-232, (2012).
36 Bumsted-O'Brien, K. M., Hendrickson, A., Haverkamp, S., Ashery-Padan, R. & Schulte, D. Expression of the homeodomain transcription factor Meis2 in the embryonic and postnatal retina. *The Journal of comparative neurology* **505**, 58-72, (2007).
37 Capdevila, J., Tsukui, T., Rodríquez Esteban, C., Zappavigna, V. & Izpisúa Belmonte, J. C. Control of vertebrate limb outgrowth by the proximal factor Meis2 and distal antagonism of BMPs by Gremlin. *Molecular cell* **4**, 839-849 (1999).
38 Sisodiya, S. M. *et al.* PAX6 haploinsufficiency causes cerebral malformation and olfactory dysfunction in humans. *Nat Genet* **28**, 214-216, (2001).